EXPERIMENTS WITH SUPERHEAVY NUCLEI*

S. HOFMANN

Gesellschaft für Schwerionenforschung (GSI)
Planckstraße 1, D-64220 Darmstadt, Germany

(Received December 1, 1998)

In two series of experiments at SHIP, six new elements ($Z = 107-112$) were synthesized via fusion reactions using lead or bismuth targets and $1n$-deexcitation channels. The isotopes were unambiguously identified by means of α-α correlations. Not fission, but alpha decay is the dominant decay mode. Cross-sections decrease by two orders of magnitude from bohrium ($Z = 107$) to element 112, for which a cross-section of 1 pb was measured. Based on these results, it is likely that the production of isotopes of element 114 close to the island of spherical *SuperHeavy Elements* (SHE) could be achieved by fusion reactions using ^{208}Pb targets. Systematic studies of the reaction cross-sections indicate that the transfer of nucleons is an important process for the initiation of fusion. The data allow for the fixing of a narrow energy window for the production of SHE using 1n-emission channels. The likelihood of broadening the energy window by investigation of radiative capture reactions, use of neutron deficient projectile isotopes and use of actinide targets is discussed.

PACS numbers: 23.60.+e, 25.70.–z, 27.90.+b

1. Introduction

At the end of the last decade, the prospects for heavy element research were not promising: Only one more decay chain of ^{266}Mt was identified in a confirmation experiment [1]. Only cross-section limits had been reached in search experiment for the elements 110 and 111 ($\sigma(^{64}\mathrm{Ni} + ^{208}\mathrm{Pb})<12$ pb [2], $\sigma(^{40}\mathrm{Ar} + ^{235}\mathrm{U})<8$ pb [3], $\sigma(^{64}\mathrm{Ni} + ^{209}\mathrm{Bi})<10$ pb [4]). Conditions for the synthesis of heavy nuclei were advanced [5], which resulted in rather pessimistic predictions for the synthesis of heavy nuclei beyond meitnerium. Reaction theory [6–10] predicted great amounts of extrapush energy necessary for the fusion of heavy ions in reactions with lead or in symmetric

* Presented at the XXXIII Zakopane School of Physics, Zakopane, Poland, September 1–9, 1998.

systems, heating the compound nucleus to several ten's of MeV, which again would lower the cross-section by compound-nucleus fission. A rapid decrease of the cross-sections far below the 1 pb level was expected for the production of new elements taking into account extrapush energy. However, an extrapolation of the experimentally known cross-sections up to element 110 showed that the 1n-emission channel of cold fusion reactions with ^{208}Pb targets resulted in the highest cross-section compared with 2n emission or hot fusion reactions. A cross-section of 1 pb was estimated for the synthesis of element 110 by the reaction ^{62}Ni + ^{208}Pb $\rightarrow$ ^{269}110 + 1n [11].

Increasing the experimental sensitivity by simply extending the measuring time was not feasible, at least not in experiments performed regularly on a cross-section level of 1 pb or less. A reduction of the measuring time could be obtained by increasing both the efficiencies of the experimental set-up and the intensity of the beam currents. Values of up to 1 pμA (1 pμA = 6.24 $\times$ 10^{12} particles/s) are feasible. In the ideal case of 100 % overall efficiency, an average of one event per day will be measured at a cross-section of 1 pb. These improved conditions would support an extension of the measurable cross-section range, down to even 0.1 pb in specific cases. The upgrades of the experimental equipment are described in more detail in Ref. [12].

2. The new elements 110, 111 and 112

A series of irradiations at SHIP using the improved set-up started at the end of 1993. The effects of the improvements were tested through the investigation of new neutron deficient isotopes of elements from mendelevium to seaborgium [13]. The reaction process was studied by measurement of excitation functions for production of rutherfordium in June-July and hassium in October 1994.

Experiments aiming at identification of elements $Z = 110$ and 111 were carried out in November-December 1994. In November-December 1995 the reaction ^{82}Se + ^{208}Pb $\rightarrow$ ^{290}116* was investigated in the search for a fusion process by radiative capture. Element 112 was identified in February-March 1996. Beams of ^{40}Ar, ^{50}Ti, ^{51}V, ^{58}Fe, ^{62}Ni, ^{64}Ni, ^{68}Zn, ^{70}Zn and ^{82}Se were used with currents up to $\approx$0.5 pμA. Targets of lead isotopes and ^{209}Bi were irradiated. The isotopes ^{269}110, ^{271}110, ^{272}111 and ^{277}112 were identified by 4, 9, 3 and 2 decay chains, respectively [12, 14]. The mean values of the decay data are shown in the chart of nuclei, Fig. 1.

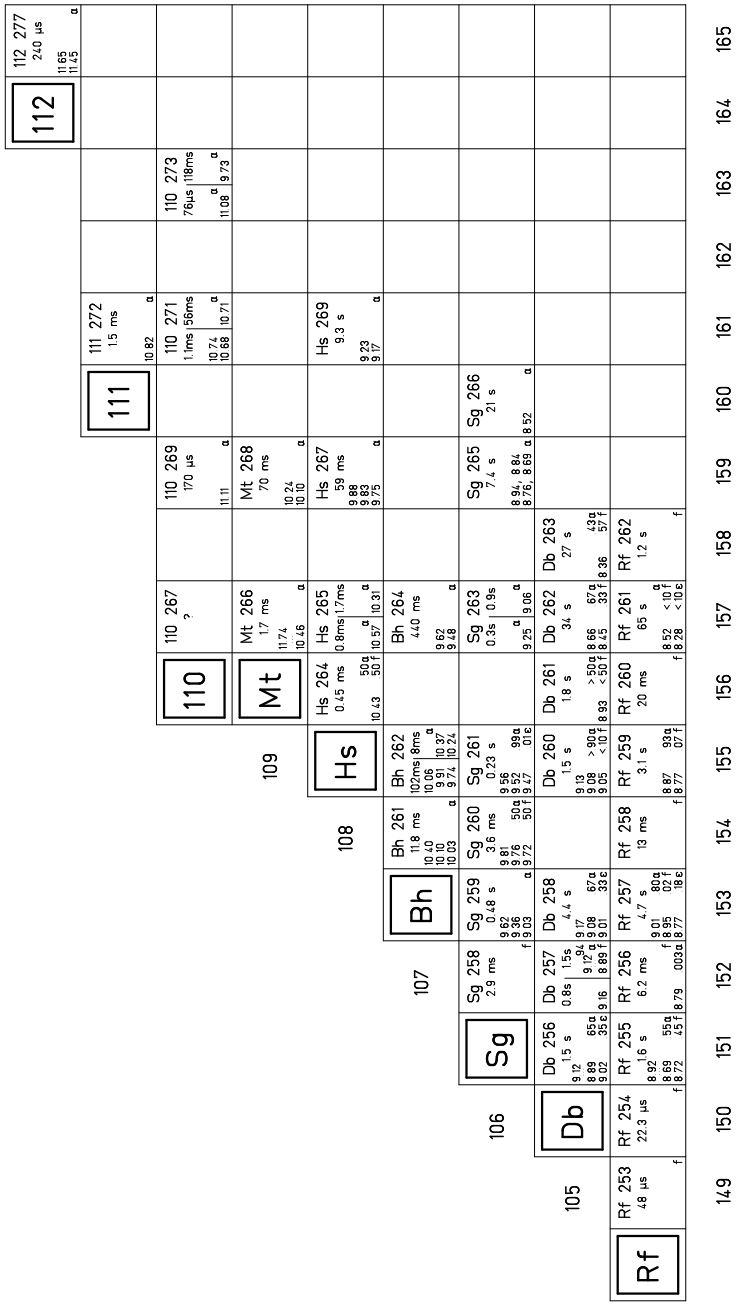

Fig. 1. The presently known isotopes of the heaviest elements. The numbers given are the total half-life, the α energy in MeV and the branching ratio for electron capture, α decay and fission.

The most neutron-rich isotopes of the elements bohrium to 110, ^{268}Mt, ^{264}Bh, ^{273}110 and ^{269}Hs could be identified as daughter products of the α decay of ^{272}111 and ^{277}112, see Fig. 1.

Shortly before the search for element 110 was initiated at SHIP, the possible evidence for observation of the α decay of ^{267}110 produced by the reaction ^{59}Co + ^{209}Bi was reported by Ghiorso *et al.* [15].

In a series of experiments the elements Sg, Hs and 110 were also investigated by a Dubna-Livermore collaboration at the U400 cyclotron at Dubna using a gas-filled separator. The hot fusion reactions ^{22}Ne + ^{248}Cm, ^{34}S + ^{238}U and ^{34}S + ^{244}Pu were studied, and the results were published by Lazarev *et al.* [16]. The data are shown in Fig. 1.

3. Search for element 113

The experiment to search for element 113 was complicated by the fact that no excitation function for the production of odd elements from dubnium ($Z = 105$) to element 111 was known well enough to allow for an estimate of the optimum beam energy for production of element 113. Therefore, the two reactions ^{58}Fe + ^{209}Bi $\rightarrow$ ^{267}Mt* [17] and ^{50}Ti + ^{209}Bi $\rightarrow$ ^{259}Db* were investigated before the main experiment. The irradiation was carried out in February and December 1997. The result of these experiments was that the position and widths of the excitation function of the 1n channel for meitnerium and of the 1n to 3n channel for dubnium are the same as for the next lighter even element, only the cross-section value is smaller.

Element 112 was observed at a ^{70}Zn-beam energy of 344 MeV, which resulted in an excitation energy of 9.85 MeV averaged over the ^{208}Pb-target thickness. To obtain the same excitation energy for production of element 113, a beam energy of 348 MeV was calculated. Using this energy, the beam time of the first part of the experiment started on March 5, 1998. Targets of ^{209}Bi with 450 μg/cm^2 thickness were irradiated. Within a period of 25 days a dose of 4.5×10^{18} projectiles of ^{70}Zn was collected, in a second period of 21 days starting at April 15, 1998, a dose of 3.0×10^{18}. A slightly different beam energy of 350 MeV was used in the second part, resulting in an excitation energy of the compound nucleus of 11.57 MeV. The obtained cross-section limits are 0.9 and 1.4 pb, respectively. The beam energy was increased slightly in the second part to take into account a possible shift of the excitation function to a higher energy, which was indicated by the two data points measured for element 111, however, with low statistical significance, The 1.7 MeV step in the excitation energy is small compared to the expected width of the excitation function so that the two limits can still be averaged. A value of 0.6 pb results at a mean excitation energy of 10.71 MeV. The cross-section limits are calculated at a probability level of 68%.

The obtained cross-section limit for the production of element 113 is not completely contradictory to the expectations. The reached limit is still higher than the lower value for the range of possible cross-sections estimated to be within a window from 0.3 to 1.0 pb. However, the experiment obviously showed that the present experimental set-up is not sensitive enough to perform regularly experiments on a level of a few hundred femtobarns within reasonable time. A further upgrade is needed in order to improve the sensitivity by another factor of 5 to 10, as it was performed in the past to reach the cross-section level of 1 pb.

4. Ground-state properties of SHE

4.1. Ground-state binding energy and deformation

Shell-model calculations based on the Strutinsky approach [18] are most successful in reproducing the measured nuclear binding energies. Experimental values are obtained by correlation of the α-decay data to decay-chain nuclei of known masses. Fig. 2 shows a plot of deviations of various calculated data from the experimental values. For odd nuclei an uncertainty in the experimental data arises, because α transitions either to excited levels or from isomeric states cannot be excluded. Such deviations may reach levels of several hundreds keV. Significant deviations of some of the calculated values of up to 3 MeV arise for nuclei, for which bigger shell gaps determine the binding energy, here at $Z = 110$, $N = 162$.

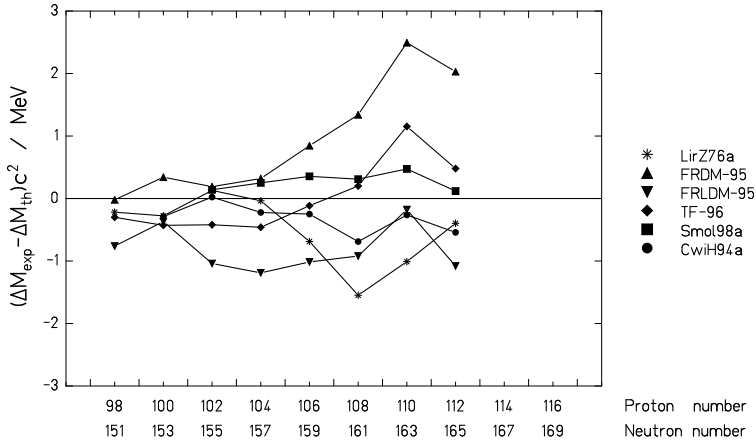

Fig. 2. Comparison of calculated mass decrements with the experimental data for nuclei of the α-decay chain of $^{277}112$. The calculated data are from Liran and Zeldes (LirZ76a) [19], Möller *et al.* (FRDM-95, FRLDM-95) [20], Myers and Swiatecki (TF-96) [21], Smolanczuk (Smol98a) [22] and Ćwiok *et al.* (CwiH94a) [23].

Recently, several attempts at understanding the shell structure properties of SHE based on the self-consistent theory were made [24,25]. There are several factors, which influence the calculations, thus making them uncertain especially in the region of SHE.

The actual location of the three low spin proton subshells $2f_{5/2}$, $3p_{3/2}$ and $3p_{1/2}$, which are filled between $Z = 114$ and 126, may result in a washing out of the shell effect for SHE. Qualitatively, we may expect a wide and less deep minimum of the negative shell-correction energies in the case that the low spin proton levels are equally distributed in energy between $Z = 114$ and 126. Then, also the fission barriers will be flat and narrow, their height and width is mainly determined by the ground-state shell-correction energy. As a result, the fission half-lives will be relatively short. On the other hand, if a wide energy gap will exist beyond one of the proton numbers 114, 120 or 126, then the shell-correction energies will be pronounced for that element. In combination with the neutron shell effect at N=184 a sharp and deep minimum will be formed, similar to that of the double magic ^{208}Pb, resulting in a high fission barrier and relatively long fission half-life. Also the α half-lives will be stronger modulated by great shell effects resulting in long α half-lives below and short half-lives above the magic number.

4.2. Decay properties of SHE

In order to estimate the decay properties of SHE, the predictions set forth by the macroscopic-microscopic models are extremely useful for the curbed extrapolation into this region. In Fig. 3 the results of the calculations by Möller *et al.* [20] and Smolanczuk and Sobiczewski [22,26] are presented.

The dominating partial half-life is shown in Fig. 4a for even-even nuclei. The two regions of deformed heavy nuclei and spherical SHE merge and form a region of α emitters surrounded by fissioning nuclei. The longest half-lives are 1000 s for deformed heavy nuclei and 30 y for spherical SHE. Nuclei with such long half-lives produced at low cross-sections ($\leq$10 nb) are difficult to measure using the present experimental techniques. In addition, only short α-decay chains are expected. The half-lives of nuclei at $N = 184$ and $Z <$110 are reduced from β^- decay.

Fig. 4b shows the presently known nuclei and compound nuclei, which could be formed by reactions with ^{208}Pb or ^{248}Cm targets and stable projectile isotopes plotted on the contour map of shell-correction energies. The region of relatively long-lived deformed heavy elements is well covered by reactions with ^{248}Cm targets or the α-decay products of reactions with ^{208}Pb targets. This is not the case for the central region of spherical SHE. The reactions ^{82}Se + ^{208}Pb $\rightarrow$ ^{290}116$*$ and ^{48}Ca + ^{248}Cm $\rightarrow$ ^{296}116$*$ result in the closest approach. Another approach may become feasible with the use of neutron-rich radioactive beams.

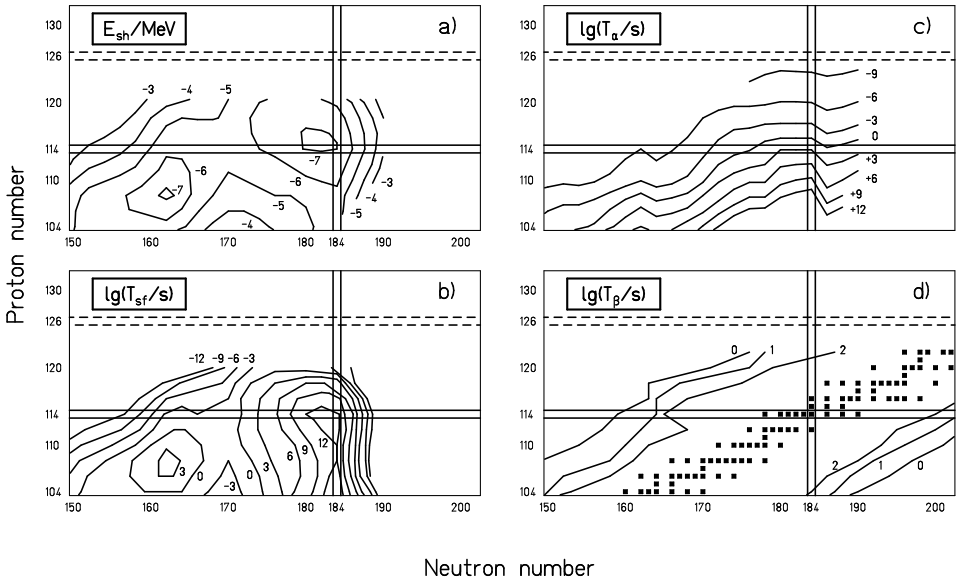

Fig. 3. The decay properties of heavy and superheavy nuclei according to macroscopic-microscopic calculations. Ground-state shell-correction energy (a); partial fission half-life of even-even nuclei (b); unhindered α-decay half-life (c); β^+ and β^- half-life (d). The β-stable nuclei are marked by filled squares. The calculated data in a), b) and c) are from Smolanczuk [22] and Smolanczuk and Sobiczewski [26] and in d) from Möller *et al.* [20].

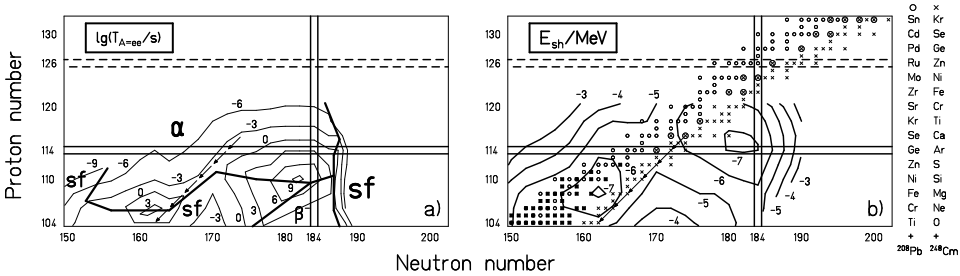

Fig. 4. Dominating partial α, β or fission half-lives for even-even nuclei (a). The bold lines separate regions of dominantly α decay, β decay and spontaneous fission. Diagram (b) shows the ground-state shell-correction energy and compound nuclei, which can be reached in reactions with targets of ^{208}Pb or ^{248}Cm and stable projectile isotopes. The presently known nuclei are marked by filled squares. The sequence of arrows indicate the hypothetical decay chain of ^{290}116.

In the case of high shell-correction energies at $Z = 126$ and $N = 184$, this region of SHE would be easily accessible with stable projectiles in both cold and hot fusion reactions with targets of lead or isotopes of the actinide elements.

5. Synthesis of SHE

5.1. Excitation functions

A summary of recently measured even-element excitation functions or cross-section values of cold fusion reactions is shown in Fig. 5. The reactions cover a range from ^{50}Ti + ^{208}Pb for the production of rutherfordium ($Z = 104$) to ^{70}Zn + ^{208}Pb for the production of element 112.

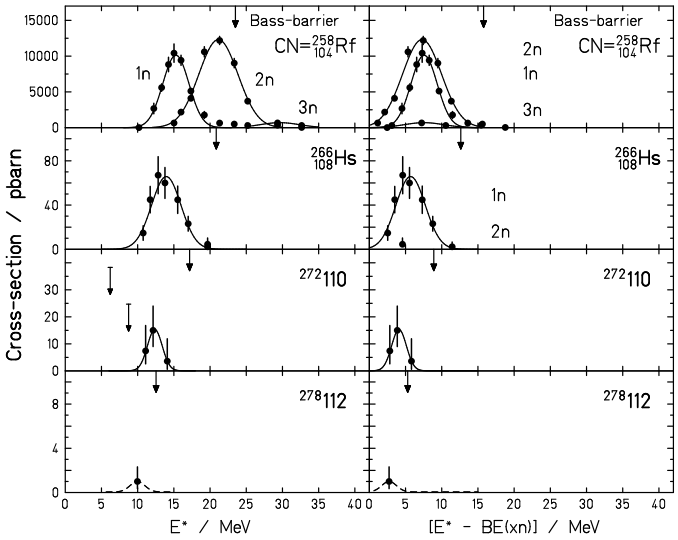

Fig. 5. Measured even-element excitation functions. On the left part, the cross-sections are plotted as a function of the dissipated energy E*, calculated from the center-of-mass beam-energies in the middle of the target thickness and the Q-values using the mass tables of Audi and Wapstra [28] for projectile and target. The mass prediction of Myers and Swiatecki [21] has been used for the compound nucleus. The arrows mark the interaction barriers of the reaction according to the fusion model by Bass [27]. On the right part, the neutron binding energies according to Myers and Swiatecki [21] are subtracted. The resulting free reaction energy is a sum of the kinetic energy of the emitted neutrons and the energy of emitted γ rays. The continuous curves are gaussian fits through the data points, the dashed curve ($Z = 112$) is extrapolated.

In all cases, where excitation functions are known, the cross-section maxima on the right in Fig. 5 are approximately centered between zero and the interaction barrier according to the Bass model [27]. This empirical result seems to present a sound means for the determination of the position of the cross-section maximum in cold fusion reactions.

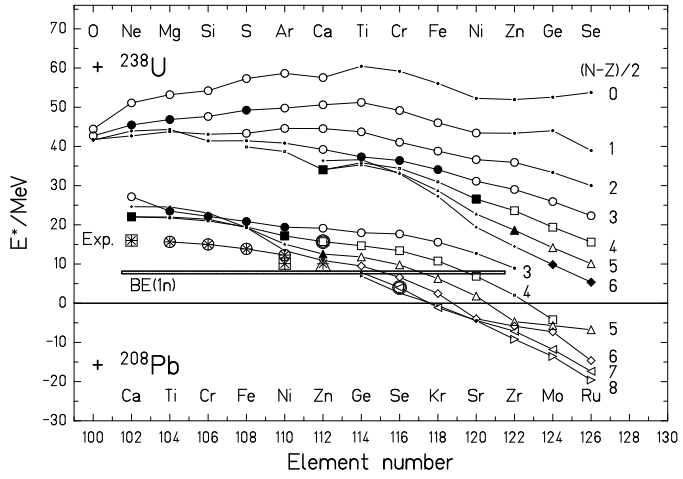

Fig. 6. Diagrams of excitation energies at the interaction barrier according the model of Bass [27]. The upper cluster shows the trend for hot fusion reactions with ^{238}U targets and projectiles between O and Se, the lower, for cold fusion reactions with ^{208}Pb targets and projectiles from Ca to Ru. For the calculation of the excitation energies see caption to Fig. 5. The large symbols mark stable projectile isotopes, the little symbols radioactive isotopes. The filled symbols of T_z=4, 5 and 6 nuclei in the upper part are enhanced, because they impressively mark the transition from hot to cold fusion with increasing element number using actinide targets. The other filled symbols up to element 112 mark reactions investigated at SHIP by cold fusion or in Dubna by hot fusion. The star symbols mark the excitation energies, at which the maximum cross-section was observed in cold fusion reactions. The 1n-binding energies of the compound-nuclei are in a range from 7.5 to 8.2 MeV, marked by the horizontal bar.

A comparison of excitation energies at the barrier for cold and hot fusion reactions over a wide range of SHE is shown in Fig. 6. A remarkable transition is observed from a region of high excitation energies (>40 MeV) for reactions with ^{238}U target resulting in elements up to ≈114 into a region of low excitation energies, down to 6 MeV for element 126. This reflects a change from hot fusion to cold fusion with regard to the excitation energy. It is however likely, that the excitation energy is not the most important quality parameter for distinguishing the two types of reaction. Another pos-

sibly more important difference could be that ^{208}Pb is a spherical closed shell nucleus with empty shells above the closure, and ^{238}U is well deformed and midshell.

Following the rule of maximum cross-sections of cold fusion reactions worked out by means of Fig. 5, the curves in fig. 6 allow for the extrapolation of the trend beyond element 112. There is only a very narrow window of excitation energy left for the production of element 114 with a ^{76}Ge beam and 1n emission.

For of element 116, the reactions with ^{82}Se and ^{80}Se already give rise to excitation energies at the barrier that are smaller than the 1n-binding energy. In this case the free energy can be emitted only by γ rays. This so called radiative capture channel was observed in SHIP experiments for heavy ions by the reaction ^{90}Zr(^{90}Zr,γ's)^{180}Hg [29]. It is not yet known in the region of SHE, where fission is a strong competition to the deexcitation of the compound nucleus.

Alternatively, the 1n channel may be investigated with neutron deficient projectiles resulting in excitation energies greater than the 1n-binding energy. This choice may become important if the reaction does not allow for an increase in the kinetic energy beyond the value determined by the Bass interaction barrier.

5.2. Fusion initiated by transfer (FIT)

In all of the investigated cold fusion reactions the largest cross-section was measured 'below the barrier'. The energy relations that determine the barrier are drawn in Fig. 7 for the reaction ^{64}Ni + ^{208}Pb and a barrier based on the model by Bass [27] is also given. A tunneling process through this barrier cannot explain the measured cross-sections. The conclusion is that additional effects must allow for fusion. Attempts to improve the heavy element fusion-barrier calculations were recently published by Möller *et al.* [30].

At and below the barrier, the kinetic energy in the center-of-mass system is converted into potential energy, and the reaction partners come to rest in a central collision in a touching configuration. In the case of ^{64}Ni + ^{208}Pb, the initial kinetic energy of 236.2 MeV, at which the cross-section maximum was measured, is exhausted by the Coulomb potential at a distance of 14.0 fm between the reaction partners. At that distance only nucleons on the outer surface are in contact.

We recall that the kinetic energy at the surface of orbiting nucleons is low. Therefore, at the point of contact of two nuclei in a central collision the probability of nucleons or pairs of nucleons leaving the orbit of one nucleus and move into a free orbit of the reaction partner is high. The process is

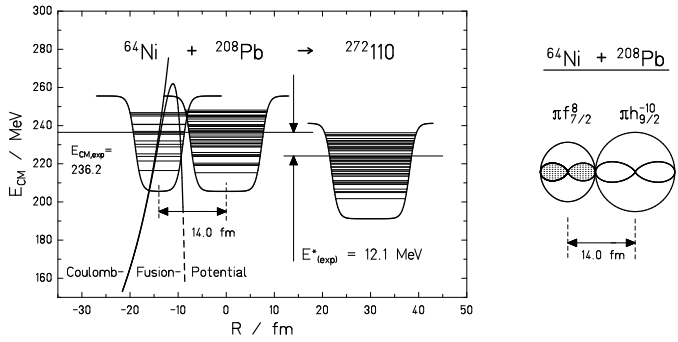

Fig. 7. Energy against distance diagram for the reaction of an almost spherical ^{64}Ni projectile with a spherical ^{208}Pb target nucleus resulting in the deformed fusion product ^{271}110 after emission of 1 neutron. At the centre-of-mass energy of 236.2 MeV the maximum cross-section was measured. On the left the reaction partners are represented by their nuclear potentials (Woods–Saxon) at the contact configuration, where the initial kinetic energy is exhausted by the Coulomb potential. On the right the outermost proton orbitals are shown at the contact point. For the projectile ^{64}Ni an occupied $1f_{7/2}$ orbit (hatched area) is drawn and for the target ^{208}Pb an empty $1h_{9/2}$ orbit. The protons circulate in a plane perpendicular to the drawing. The Coulomb repulsion, and, thus, the probability for separation is reduced by the transfer of protons. In this model the fusion is initiated by transfer (FIT).

shown schematically on the right side in Fig. 7. An adequate theoretical description could be obtained by use of the two-center shell model [31]. An approach that reproduces the measured cross-sections within the framework of a dinuclear system (DNS-model) was given by Antonenko *et al.* [32].

Because of pairing energies and high orbital angular momenta involved, the transfer of pairs is more likely than that of single nucleons. The described process is a frictionless pair transfer occurring at the contact point in a central collision at zero longitudinal momenta in the irradiation of ^{208}Pb targets. This capture process seems to already be disturbed at kinetic energies only slightly higher than those determined by the Bass interaction barrier, as discussed my means of the measured excitation functions shown in Fig. 5.

After transfer of 2 protons from ^{64}Ni to ^{208}Pb the repulsive Coulomb force is decreased by 4.9 % allowing for the maintenance of the reaction partners in close contact and for continuation of *fusion initiated by transfer* (FIT).

Important factors, which influence the cross-section at the very beginning of the fusion process, are:

1. The probability of a head-on collision.
2. The probability of proton transfer in competition with separation of the reaction partners.

The importance of cold multi-nucleon transfer for the synthesis of new elements was determined by von Oertzen [33]. The application of the FIT model in the description of the low energy fusion phenomena is based on this work and the experimental result of maximum fusion cross-sections at energies well below the Bass barrier. The transfer of massive clusters for production of heavy elements, especially neutron rich species, was considered by Magda and Leyba [34].

In the case of ^{248}Cm bombardment with ^{48}Ca the target nucleus is deformed, and at barrier energies only a fraction of certain orientations will lead to fusion. This orientation effect is absent in the case of spherical ^{208}Pb targets. In addition, the occupations of levels at the Fermi surfaces are such that protons are more likely to transfer from the target to the projectile and thus increase the Coulomb repulsion. The planned systematic irradiation of actinide targets with a ^{48}Ca beam in Dubna will probably result in basic information on the reaction process for the future synthesis of SHE by hot fusion.

6. Outlook

The recent technical developments serve as a basis for new experiments with positive results in the region of superheavy elements. Important questions are still open and need to be answered. A short list of future experiments is herewith given:

1. Proof of the shell effect at $Z = 114$ to establish the location of SHE.
2. Ground-state to ground-state α decay of even-even nuclei for more accurate evaluation of nuclear binding energies.
3. Search for α transitions of even-even nuclei into rotational levels for determination of the degree of deformation, especially in the region of nuclei near $N = 162$.
4. Fission branchings of even-even nuclei, for comparison of the extracted partial fission half-lives with the results of nuclear models.
5. Extension of the cross-section data by measurement of complete excitation functions.
6. Comparison of cross-sections of various combinations of odd and even reaction partners may be the best approach to understanding the cold-fusion reaction mechanism on a microscopic level.
7. Fusion with more neutron-rich radioactive projectiles and improved excitation-function systematics for hot-fusion reactions.
8. Search for radiative capture processes ($0n$ channel).

9. Deexcitation of the compound nucleus by in beam γ spectroscopy using the recoil tagging technique.
10. Gamma spectroscopy of separated fusion products after electron capture.
11. Trapping of separated ions for precise mass measurement and investigation of the electron configuration by laser spectroscopy.
12. Chemical properties of elements beyond seaborgium and further studies of chemical properties of seaborgium and the lighter transactinide elements.

One can hope that during the coming years more data will be measured in order to promote a better understanding the stability of the heaviest elements and the processes, that lead to fusion. Microscopic description of the fusion process may be needed for an effective explanation of the measured phenomena in the case of low dissipative energies. Then, also relationships between fusion probability and stability of the fusion products may become apparent.

An opportunity for the continuation of experiments in the region of SHE at decreasing cross-sections will be afforded by further accelerator developments. Radioactive beams and high current beams are the options for the future. At increased beam currents, values of a few 10 pμA may become possible. Ideally, the cross-section level for the performance of experiments can be shifted down into the region of 1 fb. These high currents, in turn, require the development of a new target and improvement of the separator.

For helpful discussions I want to thank S. Ćwiok, P. Möller, W. Nörenberg, W. von Oertzen and A. Sobiczewski.

REFERENCES

[1] G. Münzenberg. *et al.*, *Z. Phys.* **A330**, 435 (1988).
[2] G. Münzenberg. *et al.*, GSI Annual Report 1985, GSI-86-1, 1986, p. 29.
[3] G. Münzenberg. *et al.*, GSI Annual Report 1986, GSI-87-1, 1987, p. 14.
[4] Yu.Ts. Oganessian *et al.*, *Radiochimica Acta*, **37**, 113 (1984).
[5] K.H. Schmidt, W. Morawek *Rep. Prog. Phys.* **54**, 949 (1991).
[6] R. Nix, A.J. Sierk, *Phys. Rev.* **C15**, 2072 (1977).
[7] W.J. Swiatecki, *Nucl. Phys.* **A376**, 275 (1982).
[8] J. Blocki *et al.*, *Nucl. Phys.* **A459**, 145 (1986).
[9] P. Fröbrich, *Phys. Lett.* **B215**, 36 (1988).
[10] D. Berdichevsky *et al.*, *Nucl. Phys.* **A502**, 395c (1989).
[11] S. Hofmann, *Journal of Alloys and Compounds* **213/214**, 74 (1994).

[12] S. Hofmann, *Rep. Prog. Phys.* **61**, 639 (1998).

[13] F.P. Heßberger *et al.*, *Z. Phys.* **A359**, 415 (1997).

[14] S. Hofmann *et al.*, *Z. Phys.* **A350**, 277 (1995); **A350**, 281 (1995); **A354**, 229 (1996).

[15] A. Ghiorso *et al.*, *Nucl. Phys.* **A583**, 861c (1995); *Phys. Rev.* **C51**, R2293 (1995).

[16] Yu.A. Lazarev *et al.*, *Phys. Rev. Lett.* **73**, 624 (1994); *Phys. Rev. Lett.* **75**, 1903 (1995); *Phys. Rev.* **C54**, 620 (1996).

[17] S. Hofmann *et al.*, *Z. Phys.* **A358**, 377 (1997).

[18] V.M. Strutinsky, *Nucl. Phys.* **A95**, 420 (1967).

[19] S. Liran, N. Zeldes, *Atomic Data and Nucl. Data Tables* **17**, 431 (1976).

[20] P. Möller *et al.*, *Atomic Data and Nucl. Data Tables* **59**, 185 (1995).

[21] W.D. Myers, W.J. Swiatecki, *Nucl. Phys.* **A601**, 141 (1996).

[22] R. Smolanczuk, *Phys. Rev.* **C56**, 812 (1997), and private communication, August 1998.

[23] S. Ćwiok *et al.*, *Nucl. Phys.* **A573**, 356 (1994).

[24] S. Ćwiok *et al.*, *Nucl. Phys.* **A611**, 211 (1996).

[25] K. Rutz *et al.*, *Phys. Rev.* **C56**, 238 (1997).

[26] R. Smolanczuk, A. Sobiczewski *Proceedings of the XV. Nuclear Physics Divisional Conference on Low Energy Nuclear Dynamics*, St.Petersburg, Russia, April 18-22, 1995, World Scientific, Singapore 1995, p. 313-320.

[27] R. Bass, *Nucl. Phys.* **A231**, 45 (1974).

[28] G. Audi, A.H. Wapstra, *Nucl. Phys.* **A565**, 65 (1993).

[29] J.G. Keller *et al.*, *Z. Phys.* **A311**, 243 (1983).

[30] P. Möller *et al.*, *Z. Phys.* **A359**, 251 (1997).

[31] D. Scharnweber *et al.*, *Z. Phys.* **A228**, 257 1971.

[32] N.V. Antonenko *et al.*, *Phys. Rev.* **C51**, 2635 (1995).

[33] W. von Oertzen, *Z. Phys.* **A342**, 177 (1992).

[34] M.T. Magda, J.D. Leyba, *Int. J. Mod. Phys.* **E1**, 221 (1992).